Computational investigation of projector lenses using mathematical models

Sami Gumaan Salmen Daraigan[a], Hassan Nouri Abdulb-Wahab Al-Obaidi[b] and Mohd Zubir Matjafri[c]
[a]*Faculty of Science, Department of Physics, Hadhramout University of Science and Technology (HUST), Mukalla, Yemen*
[b]*College of Education, Department of Physics, Al-Mustansiriyah University, Baghdad, Iraq*
[c]*School of Physics, Universiti Sains Malaysia, 11800 Penang, Malaysia*

(Received 10 August 2009)

In this paper, a computational technique for the limit of performance of the projector lenses that reconstructed using analytical functions has been carried out successfully. The projector optical properties of imaging magnetic fields of these lenses have been evaluated and hence compared. Considerable attention has been given for the objective and practical uses of such lenses. The results have shown clearly that some of these lenses are more advantageous than their counterpart.

I. INTRODUCTION

It is well known that each electron lens which is the basic constituent of any charge – particle column has two different sorts electron optical properties, namely objective and projector (asymptote). The domination of any of these types of properties depend on the function of the lens, where the objective has a considerable importance when a such lens is used as an objective lens, while the asymptote become the main factor that limit performance of the lens when it is used as a projector lens. However, the most important objective defects are spherical and chromatic aberrations, whereas the radial and spiral distortions are the main defects that deteriorate the quality of the projector lens.

Projection system can and usually does introduce distortion into the image. This sort of aberration detracts only from faithfulness, but not from the sharpness of image. For both the intermediate and projector magnetic electron lenses, radial and spiral distortions are the most important [1]. Since all of the projector defects in electron lenses can be corrected are eliminated, see for example [2-6]. While the spherical and chromatic aberrations can vanish most of the optimization approaches (especially the synthesis) are concerned only with objective defects. In fact, it is important to determine the projector defects of the target functions which had been proposed previously by others simultaneously with that of the well known mathematical models and comparing the results. This is, however, the objective of our study.

II. THE MATHEMATICAL MODEL

In order to perform a rapid and approximate evaluation of lens properties without actually caring out a detailed analysis the axial field (or potential) distribution is given by a mathematical model i.e. can approximation for the axial field (or potential) distribution that is reasonably close to the real one and allows a solution in closed form or approximation in simple terms [7]. So for, several models have been proposed to and approximate the axial magnetic field distribution for the symmetrical magnetic lenses. Most of them are presented in this work and characterized by two main factors namely; the half-width a and the maximum magnetic field i.e. the peak value, B_0. The mathematical (axial magnetic field) distribution of these models is as follows;

(a) Glaser's bell-shaped model [8];

$$B_z(z) = B_0[1.0 + (z^2/a)^2]^{-1}. \quad (1)$$

(b) Grivet–Lenz model [9];

$$B_z(z) = B_0 \operatorname{sech}[2.624(z/z)]. \quad (2)$$

(c) Exponential field model [10];

$$B_z(z) = B_0 \exp[-(\ln 2/a)z]. \quad (3)$$

(d) Gaussian field model [9];

$$B_z(z) = B_0 \exp[-(2z/a)^2 \ln 2]. \quad (4)$$

(e) Spherical polepiece model [9];

$$B_z(z) = B_0(3.847)^3[3.847 + (2z/a)]^{-3}. \quad (5)$$

(f) Cosine field model [11];

$$B_z(z) = B_0 \cos^n[(\delta/a)2z] \quad (6)$$

where $\delta = \cos^{-1}(0.5)^{1/h}$ and n is the shape factor of the cosine field.

g) Hyperbolic tangent model: This model have been proposed to represent the magnetic scalar potential distribution in the symmetrical magnetic lenses [12]. According the corresponding magnetic imaging field can be written as shown in the following formula;

$$B_z(z) = B_0 \operatorname{sec} h^2[2.270(z/a)]. \quad (7)$$

h) The inverse hyperbolic sine model: Similarly, the model was proposed to approximating magnetic scalar potential for long symmetrical magnetic lenses, [13]. However, from which one can deduce the magnetic imaging field to be;

$$B_z(z) = B_0 /[1.0 + 3(2z/a)^2]^{\frac{1}{2}} \quad (8)$$

It should be mentioned that, some of the suggested models to approximate such target functions are found to be anther mathematical image of the well known mathematical model. For example the inverse tangent function which was used to represent the scalar potential [14] is found to be a differential image for the Glaser's bell-shape model.

III. RESULTS AND DISCUSSION

Fig. 1 shows the axial magnetic field distribution belonging to each mentioned model at constant values of B_0, a and lens length L. Owing to the field profile, one can see that the Inverse hyperbolic sine model has a longer extension while the Cosine model has a shorter extension along the optical axis. However, the remaining models have an extension arranged between those two limits. Thereby, one can initially decide that the former model produced a long lens while the lateral one product a short lens.

The projector focal length (f_p) as a function of the excitation parameter $NI/\sqrt{V_r}$ for each model are plotted in Fig. 2. It is seen that each (f_p) curve has a single minimum value differ in its magnitude and position from their counter part. The models of inverse hyperbolic sine and cosine have the larger and smaller values of $(f_p)_{\min}$ respectively while the reaming models have $(f_p)_{\min}$ values graduating from the inverse hyperbolic to the cosine as shown in Table I. This result demonstrate an important fact in electron optics, that as long as the B_0 and a maintain constant the refractive power of the imaging field distribution will increase whenever its localization increases. Fig. 3, however, refocus conclusion where it is rival that the refractive power at the value of $(f_p)_{\min}$ is much higher for Cosine field model than that of the other models.

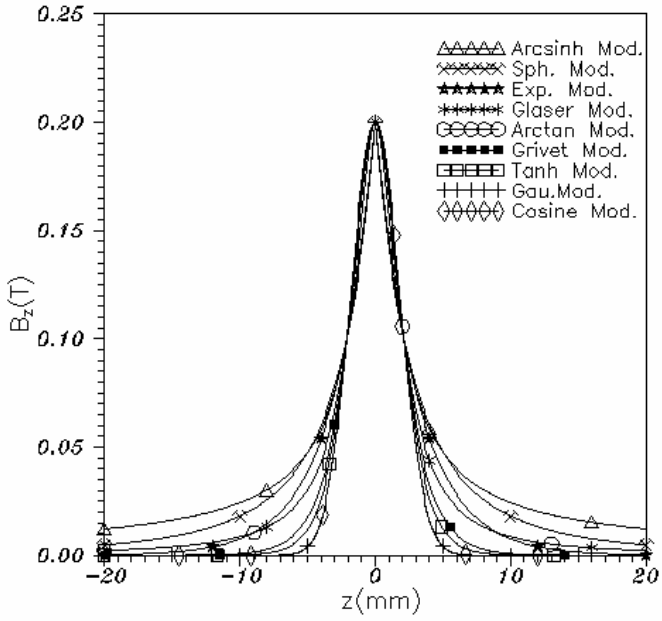

FIG. 1. The axial magnetic field distribution for various models at (B_0 = 0.2*T*, *a* = 4.230 mm, *L* = 40 mm).

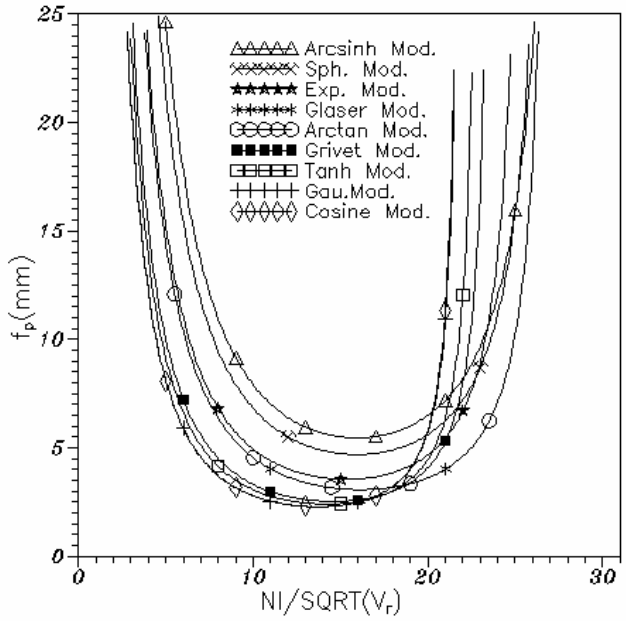

FIG. 2. The variation of the projector focal length f_p versus the excitation parameter $NI/\sqrt{V_r}$ for each distribution.

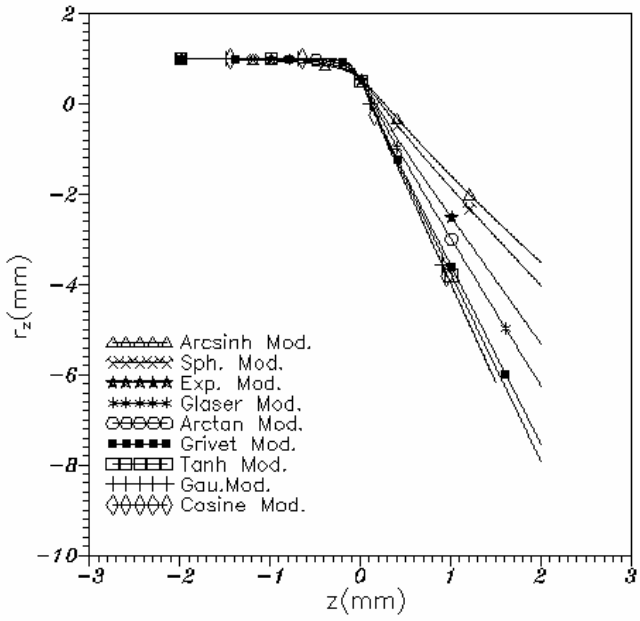

FIG. 3. The electron trajectory a long the optical interval $-3 \le z \le 3$ for each model at $(f_p)_{\min}$.

TABLE I. Several important parameters for each considered mathematical model at ($B_0 = 0.2T$, $a = 4.230$ mm, $L = 40$ mm).

Model	NI (A.t)	$(f_p)_{\min}$ (mm)	$NI/\sqrt{V_r}$ at $(f_p)_{\min}$	at D_r $NI/\sqrt{V_r}$ at $(f_p)_{\min}$	at D_s $NI/\sqrt{V_r}$ at $(f_p)_{\min}$	Q_r	Q_s	$NI/\sqrt{V_r}$ at $D_r = 0$
Arcsinh	20.10	1.151	0.962	0.045	0.031	15.90	5.457	1356.54
Sph.	18.80	1.122	0.801	0.057	0.029	16.00	4.685	1186.66
Exp.	17.10	1.094	0.625	0.095	0.030	15.40	3.542	969.87
Glaser	18.00	1.105	0.601	0.130	0.038	16.20	3.066	986.57
Arctan	18.00	1.105	0.601	0.130	0.038	16.20	3.066	986.57
Grivet	15.50	1.071	0.466	0.180	0.034	14.60	2.524	802.96
Tanh	14.90	1.063	0.423	0.196	0.031	14.20	2.402	763.84
Gau.	14.00	1.059	0.322	0.216	0.020	13.70	2.279	716.62
Cosine	14.00	1.061	0.307	0.218	0.018	13.70	2.275	714.77

(Sph. = Spherical, Exp. = Exponential, Gau. = Gaussian)

The radial and spiral distortion parameters (Q_r and Q_s) as a function of the $NI/\sqrt{V_r}$ are plotted in Figs. 4 and 5 respectively. It is clear that those curves have a conventional behavior where each curve reduces from higher values again due to the behavior of f_p curve. Thereby, the quality of the considered models are arranged from the Inverse hyperbolic sine (minimum quality) to the Cosine field (higher quality) inspect of the higher value of the spiral distortion coefficient D_s for the Cosine field in comparison with other models, see Table I and Fig. 6. Concerning the value $NI/\sqrt{V_r}$ at which the radial distortion coefficient D_r vanishes and $NI/\sqrt{V_r}$ at which f_p become minimum, the Cosine field and Gaussian models have rising better in comparison with their counter part. Where the values of those two parameters approximately the same for the Cosine and Gaussian models while the deviation between them become larger and larger as one moves from this two models to the Inverse hyperbolic sine model as Table I indicate. This means, however, a radial distortion free images at the first maximum magnification in Cosine field and Gaussian models one can obtain.

Fig. 7 shows the reconstructed polepieces shapes for each B_z distribution plotted in Fig. 1. The bore diameter and the air-gap width of each polepiece in this figure are listed in Table II. The third column represent the values of S were measured from the same point, that used to determine the value D, to the symmetry plane $(z = 0)$. While the fourth column represent the air-gap width which measured as a nearest axial distance between the faces two polepieces. However, the fifth and sixth columns shows the geometrical constant L calculated from the relation [15]:

$$L = (S^2 + 0.56D^2)^{0.5} \tag{9}$$

for both descriptions of S. According to the lateral reference the value of minimum projector focal length can be estimated experimentally by the formula:

$$(f_p)_{\min} = 0.55L\,. \tag{10}$$

It is seen that each of the relation $(f_p)_{\min}/L$ and $(f_p)_{\min}/L'$ has a different behavior especially when the corresponding B_z distribution becomes of a shorter extension a long the optical axis .Where it can be seen that the deviation of these two relation from the experimental result (0.55) increases as the B_z excitation a long the optical axis increase. From anther point of view, it can be say that this deviation increases as the curvature of the pole face (i.e. the difference between S and S') increases. Finally it should be mention that, the experimental relation [16]

$$a = 0.97L \tag{11}$$

failed entirely for the present calculations.

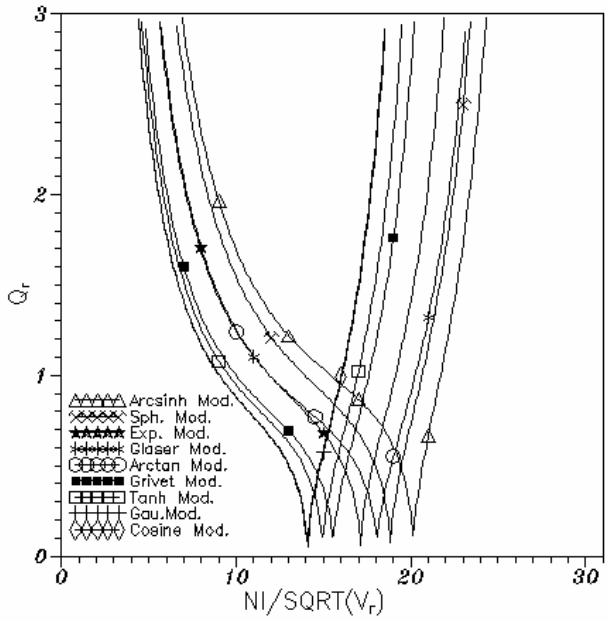

FIG. 4. The radial distortion parameter Q_r as a function of the excitation parameter $NI/\sqrt{V_r}$ for each distributions.

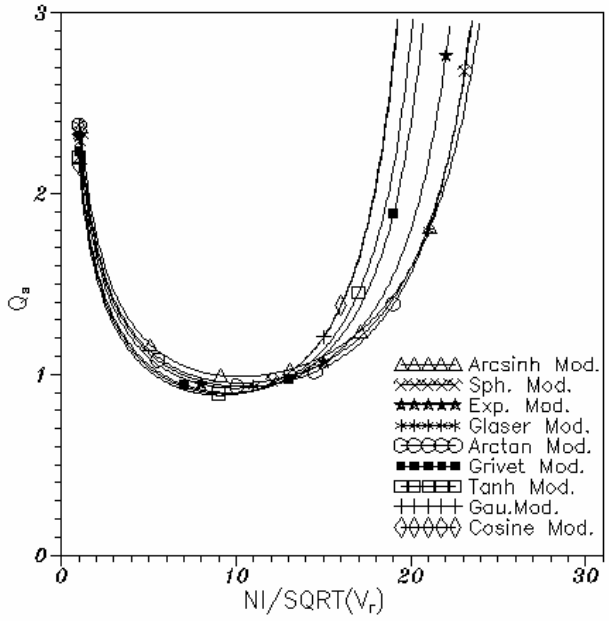

FIG. 5. The spiral distortion parameter Q_s as a function of the excitation parameter $NI/\sqrt{V_r}$ for each distributions**.**

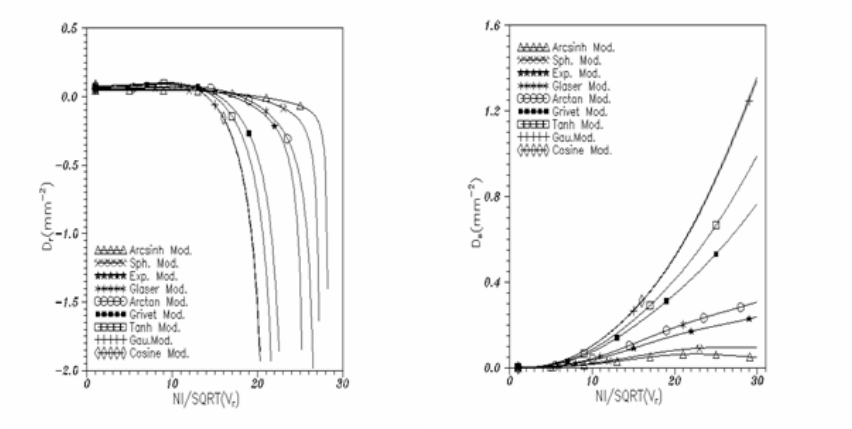

(a) (b)

FIG. 6. The variation of the: (a) radial distortion coefficient D_r , and (b) spiral distortion coefficient as a function of the excitation parameter $NI/\sqrt{V_r}$ for each distributions.

TABLE II. The geometrical parameters for each mathematical model.

Model	D (mm)	S (mm)	S' (mm)	L (mm)	L' (mm)	$(f_p)_{\min}/L$ (mm)	$(f_p)_{\min}/L'$ (mm)
Arcsinh	14.0	2.2	0.4	10.710	10.48	0.510	0.521
Sph.	13.2	0.6	0.4	9.896	9.886	0.473	0.474
Exp.	12.2	0.8	0.4	9.167	9.138	0.386	0.388
Glaser	9.8	4.0	0.6	8.354	7.360	0.367	0.417
Arctan	9.8	4.0	0.6	8.354	7.360	0.367	0.417
Grivet	6.4	16.0	0.6	16.701	4.830	0.144	0.523
Tanh	4.8	22.0	1.6	22.291	3.930	0.108	0.612
Gau.	1.6	16.8	2.0	16.843	2.330	0.135	0.978
Cosine	1.6	16.8	2.0	16.843	2.330	0.135	0.976

IV. CONCLUSION

The Cosine field and Gaussian models can be used to build up projector magnetic lenses of favorable properties in comparison with any magnetic field model. Furthermore, such lenses have a feature that they are a short and required a low a pertain energy.

The well known experimental relationships in electron optics that obtained from the analysis procedure, is no longer valid for the reconstructed lenses in the synthesis procedure, since there are several restrictions in the analysis procedure will not be found in the synthesis. In addition, from this study is proved that the presented technique has very high accuracy for design of electron lenses.

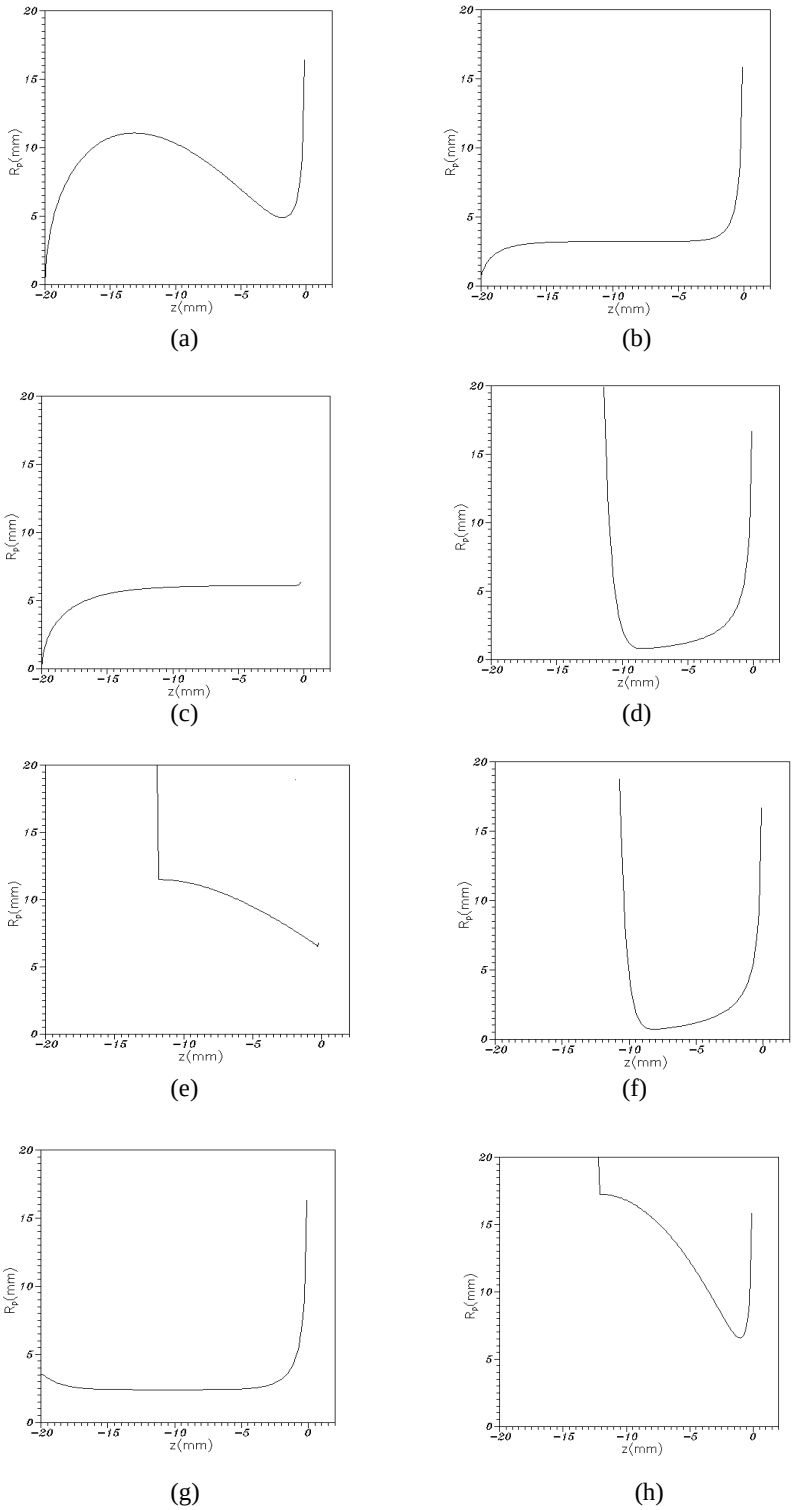

FIG. 7. The polepieces shape for: (a) Glaser's bell-model (Inverse tangent model); (b) Grivet-Lenez model; (c) Exponential field model; (d) Gaussian field model; (e) Spherical polepiece model; (f) Cosine field model; (g) Hyperbolic tangent model; (h) Inverse hyperbolic sine model.

REFERENCES

[1] A. S. A. Alamir, "Spiral distortion of magnetic lenses with fields of the form $B(z)/z^n$, $n = 2,3,4$ ", Optik, **114(12)**, 525-528 (2003)

[2] J. Hillier, "A study of distortion in electron microscope projector lenses", J. Appl. Phys., **17**, 411-419 (1946).

[3] P. Grivet, *Electron Optics*, Pergamon Press, Oxford (1972).

[4] F. Z. Marai and T. Mulvey, "Scherzer's formula and the correction of spiral distortion in the electron microscope", Ultramicroscopy, **2**, 178-192 (1977).

[5] H. N. Al-Obaidi, *Determination of the Design of Magnetic Electron Lenses Operated Under Pre-assigned Magnification Condition*, Ph. D. Thesis, Baghdad University, Baghdad, Iraq (1995).

[6] A. K. Al-Saadi, *Computations On The Properties of Magnetic Doublet Lenses for the Transmission Electron Microscope*, Ph. D. Thesis, Al-Mustansiriyah University, Baghdad, Iraq (1996).

[7] M. Szilagyi, *Electron and Ion Optics*, Plenum Press, New York (1988).

[8] Y. Kang, T. Tang, Y. Ren and X. Guo, "Differential algebraic method for computing the high order aberrations of practical electron lenses", Optik, **118**, 158-162 (2007).

[9] H. N. Al-Obaidi, I. S. Al-Nakeshli and S. M. Juma, "Computer-aided synthesis of symmetrical magnetic lenses", J. Col. Edu., Al-Mustansiryah University, **2**, 21-30 (1999).

[10] P. W. Hawkes, *Magnetic Electron Lenses*, Springer-Verlag, Berlin (1982).

[11] H. N. Al-Obaidi, "A new analytical mathematical model for approximating the magnetic field of symmetrical lenses", J. Col. Edu., Al-Mustansiriyah University, **3**, 35-46 (1999).

[12] H. N. Al-Obaidi, A. K. Al-Saadi and S. A. Mahdy, "Optimization of magnetic lens using hyperbolic tangent function", J. Col. Edu., Al-Mustansiriyah University, **1**, 87-99 (2001).

[13] S. G. Daraigan, *Computer Aided-Synthesis of Electron Lenses Using A Preassigned Analytical Functions*, M. Sc. Thesis, Col. Edu. Al-Mustansiriyah University, Baghdad, Iraq (2001).

[14] H. N. Al-Obaidi and S. G. Daraigan, "Synthesis of the symmetrical double polepiece magnetic lenses using analytical functions", Proc. 14th Conf. Cd. Col. Edu., Al-Mustansiriyah University (2001).

[15] T. Mulvey and M. J. Wallingten, "Electron lenses", Rep. Prog. Phys., **36(4)**, 347-421 (1973).

[16] G. R. Fert and P. Durandeau, *Magnetic Electron Lenses, Focusing of Charged Particles*, 1 edn. by A. Septier, Academic, New York (1967), 309-352.